IET Generation, Transmission & Distribution

Research Article

Efficient energy management for a grid-tied residential microgrid

ISSN 1751-8687
Received on 20th July 2016
Revised 24th January 2017
Accepted on 24th April 2017
E-First on 25th April 2017
doi: 10.1049/iet-gtd.2016.1129
www.ietdl.org

Amjad Anvari-Moghaddam[1] ✉, Josep M. Guerrero[1], Juan C. Vasquez[1], Hassan Monsef[2], Ashkan Rahimi-Kian[2]

[1]Department of Energy Technology, Aalborg University, 9220 Aalborg East, Denmark
[2]School of ECE, College of Engineering, University of Tehran, Tehran, Iran
✉ *E-mail: aam@et.aau.dk*

Abstract: In this study, an effective energy management system (EMS) for application in integrated building and microgrid system is introduced and implemented as a multi-objective optimisation problem. The proposed architecture covers different key modelling aspects such as distributed heat and electricity generation characteristics, heat transfer and thermal dynamics of sustainable residential buildings and load scheduling potentials of household appliances with associated constraints. Through various simulation studies under different working scenarios with real data, different system constraints and user's objectives, the effectiveness and applicability of the proposed model are studied and validated compared with the existing residential EMSs. The simulation results demonstrate that the proposed EMS has the capability not only to conserve energy in sustainable homes and microgrid system and to reduce energy consumption costs accordingly, but also to satisfy user's comfort level through optimal scheduling and operation management of both demand and supply sides.

Nomenclature

$H(\cdot)$	heaviside step function

Sets

h	index of time
M	set of non-schedulable tasks
N	set of schedulable tasks
T	set of time intervals in a given day
T_v	set of time intervals in a valid optimisation period

Parameters

A	WT rotor swept area (m^2)
A_{cloth}	surface area of a clothed person (m^2)
A_f	floor area on the sunny side of the building (m^2)
A_s	exposed surface area (m^2)
A_{st}	surface area of a hot water storage tank (m^2)
C_p	WT efficiency coefficient
$c_{p,f}$,$c_{p,I}$	specific heat capacity coefficient of the floor and the indoor air [J/(kg °C)]
E_{BESS}	battery energy capacity (kWh)
f_{load}	load factor of a motor during operation (%)
f_{PV}	PV derating factor (%)
F_r	radiation factor of a cooking appliance (%)
F_u	usage factor of a cooking appliance (%)
f_{usage}	motor usage factor (%)
G_{ref}	nominal gas consumption rate for producing 1 kWh energy (m^3/kWh)
G_T, $G_{T,STC}$	solar radiation incident on PV in real and test conditions (kW/m^2)
h_{conv}	convection heat transfer coefficient (W/(m^2 °C))
h_o	combined convection and radiation heat transfer coefficient (W/(m^2 °C))
h_{rad}	radiation heat transfer coefficient (W/(m^2 °C))
HWD	hot water demand (l)
I	direct solar radiation (W/m^2)
m_d, m_r	active-droop constants of the VCM and PCM units [(rad/s)/W]
m_f, m_i	mass of the floor and the indoor air (kg)
n_d, n_r	reactive-droop constants of the VCM and PCM units [(rad/s)/VAr]
$\bar{P}_D$	maximum power consumption of a house (kW)
$\bar{P}_{ch}$, $\bar{P}_{dch}$	battery maximum charging and discharging powers (kW)
$\bar{P}^e$, $\underline{P}^e$	upper and lower limits on a µCHP electrical output (kW)
$\bar{P}^{th}$, $\underline{P}^{th}$	upper and lower limits on a µCHP thermal output (kW)
P_D^{th}	heat demand (kW)
P_{ramp}^e	maximum allowable µCHP electrical ramp rate (kW/h)
P_{ramp}^{th}	maximum allowable µCHP thermal ramp rate (kW/h)
ΔT_{th}	threshold temperature difference (°C)
P_n	rated power of a motor (kW)
R_{cloth}	unit thermal resistance of clothing ((m^2 °C)/W)
$R_{combined}$	combined resistance ((m^2 °C)/W)
R_{st}	thermal resistance of the HWST ((m^2 °C)/W)
SAF	lighting special allowance factor
SF	space fraction (%)
T_b	basement temperature (°C)
T_c, $T_{c,STC}$	PV cell temperature at real and test conditions (°C)
T_{cw}	entering cold water temperature (°C)
T_{eq}	mean radiant and ambient temperatures (°C)
T_{out}	outdoor temperature (°C)
T_{set}	user-specified set-point for indoor temperature (°C)
T_{surr}	average surrounding surface temperature (°C)
U	overall heat transfer coefficient (W/(m^2 °C))
UF	lighting usage factor (%)
V	wind velocity (m/s)
V_{tot}	total HWST volume (l)
Y_{PV}	nominal output of a PV array (kW)
α_f	solar absorptivity of the house floor (%)

α_p	temperature coefficient of power for a PV system (%/°C)
α_s	solar absorptivity of the exposed surface (%)
β	blade pitch angle (deg)
γ	penalty factor for user's comfort level adjustment
δ	user's subscription rate (%)
Δh_{step}	examined time step (h)
ΔT_{th}	threshold temperature difference (°C)
ε	emissivity of the exposed surface (%)
$\zeta_{1,2}$	weighting coefficients
η_{ch}, η_{dch}	battery's charging and discharging efficiencies (%)
η_e, η_{th}	electric and thermal efficiency of a μCHP unit (%)
η_{fg}	enthalpy of water vaporisation (kJ/kg)
η_{motor}	motor efficiency (%)
η_H, η_C	heating and cooling performance coefficients
λ	tip speed ratio
μ_{evap}	evaporation rate from a body (kg/s)
ρ	air density at WT site (kg/m^3)
ρ_{gas}	natural gas price (cent/m^3)
σ	Stefan–Boltzmann constant [W/(m^2 °C]).
ψ	penalty factor for user's satisfaction degree adjustment

Variables

CL	thermal comfort level of inhabitants
E, E^*	output voltage of VCM and PCM converters (V)
E_g	measured point of common coupling voltage (V)
g_{CHP}, g_{aux}	total gas flow into the FC and auxiliary boiler systems (m^3/h)
P, P^*	active power output of VCM and PCM converters (kW)
P_{grid}	exchanged power with utility (kW)
P_{RH}	power consumption of a heat pump (kW)
P_{BESS}^{ch}	charging power of the battery (kW)
P_{BESS}^{dch}	discharging power of the battery (kW)
P_{aux}^{th}	thermal power output of auxiliary boiler (kW)
P_{loss}^{th}	heat loss of HWST (kW)
Q, Q^*	reactive power output of VCM and PCM converters (kVAr)
Q_{fg}	heat flow between the house floor and the ground (kW)
Q_{fi}	heat flow between the house floor and the inside air (kW)
Q_{ihg}	internal heat gain of a building (kW)
Q_{io}	heat flow between the indoor air node and the outdoor environment (kW)
Q_{occ}	heat generated by the occupants (kW)
Q_{RH}	heat output of the RFH/CS (kW)
Q_{si}	heat flow between the exposed surfaces and the inside air node (kW)
Q_{st}	energy content of the HWST (kW)
$s_i\,(h)$	binary variable showing the on/off state of appliance i at time h
$SL_i(h)$	occupant satisfaction degree once device i is operated at time h
SOC	battery state of charge (%)
T_f	house floor temperatures (°C)
T_{in}	indoor air temperatures (°C)
T_{skin}	average skin temperature (°C)
u_{aux}	ON/OFF state of auxiliary boiler (1: ON, 0: OFF)
u_{BESS}	binary variable showing the battery status (‘1’ = charging and ‘0’ = discharge)
u_{CHP}	ON/OFF state of μCHP (1: ON, 0: OFF)
u_{RH}	status of RFH/CS (‘1’: heating, ‘0’: cooling)
ω, ω^*	frequency of VCM and PCM converters (rad/s)
ω_g	measured grid frequency (rad/s)

1 Introduction

Average energy consumption distribution in different sectors at the worldwide level illustrates that more than one-third of total consumption in each society is contributed to the residential buildings [1, 2]. Although the rising rate of energy consumption in this sector has slowed down recently thanks to the energy-aware solutions, the energy price is still going up [3, 4]. In this regard, many ongoing research activities are directed towards energy efficiency in residential buildings and its impact on environment and climate [5–10]. Accordingly, a large number of initiatives have also been taken into account for the promotion of sustainable consumption and green living patterns as well as delivery of affordable clean and reliable power to customers which in turn necessitates the use of smart building automation and energy management solutions. Although ‘energy management’ is a term that has a number of meanings, in this paper we concern about the process of energy auditing and optimal scheduling of energy sources in a given organisation here called as integrated building and microgrid systems or residential microgrids. With regard to this terminology and in the way to address emerging challenges and the gaps in this area, extensive research programmes have been initiated recently and many researchers around the world have elaborated on that [11–29]. For example, a building energy management system is proposed in [11] to enable users to monitor, manage and control the energy used in their own buildings, thus reducing the demand and energy consumption costs. Similar smart energy management system is outlined in [12], where a day-ahead scheduling algorithm is utilised for managing different distributed energy resources at each time with regard to minimum operation cost of the microgrid. An optimal energy scheduling for a residential grid-tied microgrid supplemented by battery energy storage systems (BESSs) is developed in [13] and a computationally efficient algorithm for determining the optimal exploitation of energy sources from economic perspectives is proposed thereafter. A penny-wise algorithm for energy management in a home environment is proposed in [14] considering real-time pricing (RTP) for electricity consumption. Another cost-efficient residential load scheduling framework is introduced in [15] paying no attention to the optimal control and management of in-home generation devices that can support further reduction of end-use energy costs. Similar demand scheduling and energy management strategies are also developed in [16–22] for residential/office buildings, in [23–25] for energy hubs and small- to medium-size microgrids, and in [26–29] for integrated smart homes/buildings and microgrid systems.

Based on the reviewed literature, it can be easily understood that there exist numerous research works that have tackled the energy management problem in residential microgrids with regard to different objectives and points of functionality. However, electrical/thermal energy costs together with the consumers’ comfort levels are not considered as two key objectives in developing an efficient energy management system (EMS) for such integrated energy systems (IESs) or any similar systems that could provide active participation of prosumers as informed users. Moreover, most of mentioned works have mainly proposed a system-level strategy for EMS design and operation which neglects the interaction between system-level components and lower-level controllers. Last but not least, very few works have considered thermal dynamics of a building unit while drawing working plan for energy management within a residential section.

In this paper, an optimal energy management model for a residential microgrid with various types of distributed energy sources and intelligent household devices is proposed. To satisfy user's need in terms of reduced energy costs and improved comfort levels in an integrated optimisation problem, first the mathematical models of the targeted residential microgrid components are presented. Then, methods for quantitative measurements of the users’ satisfaction degrees and comfort levels are presented; and finally the optimal control policy with active participation of both generation and demand sides under various working environments and conditions will be configured and validated. The main contributions of this paper could be summarised as follows:

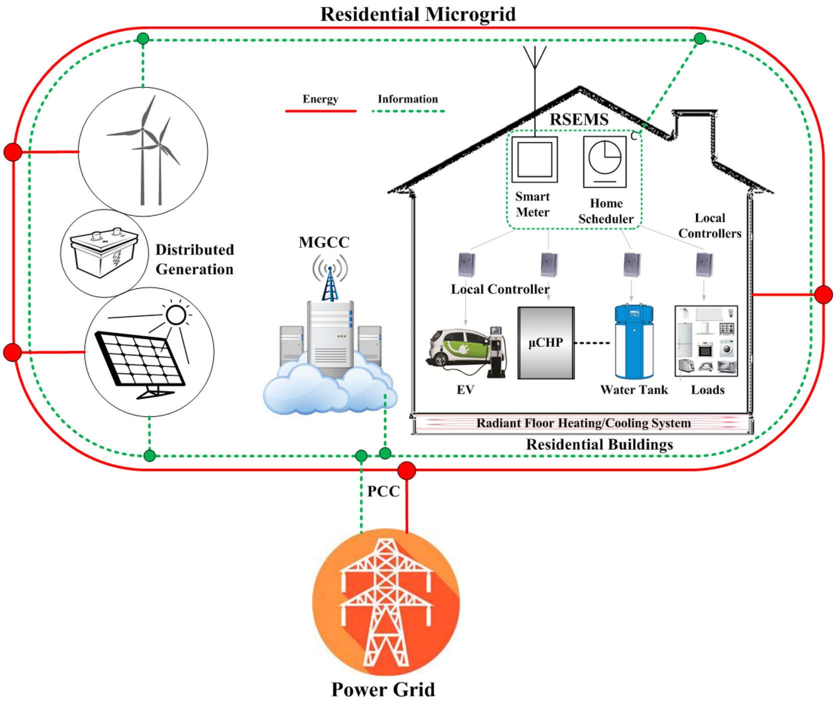

Fig. 1 *Integrated building and microgrid system*

- Coordinated system-level energy management and lower-level supply/demand side control is proposed according to energy and comfort management in an IES.
- Optimal operation and hierarchical control of dispersed generation (DG) units are proposed in the context of AC microgrids.
- Heat dynamics of a residential building unit is improved through incorporation of different internal/external heat sources.

The rest of this paper is organised as follows. Section 2 describes the configuration and specifications of the proposed system. Section 3 introduces the mathematical model of the system components. Evaluation of the proposed residential smart EMS (RSEMS) for several practical operating scenarios is performed in Section 4, and Section 5 concludes this paper and discusses future works.

2 System configuration and specification

A block diagram of the proposed integrated building and microgrid system is shown in Fig. 1. On the generation side, the main actors include the utility (power grid) and the controllable DGs such as micro-combined co-generation system (µCHP), while in demand side, schedulable appliances serve as actors.

In the proposed structure, the leading actor is the RSEMS that manages the operation of in-home devices and appliances optimally in coordination with microgrid central controller taking into account users' objectives and existing technical/operational constraints. RSEMS also provides required information such as set-points and reference signals for local controllers when it is needed. While the RSEMS is designed as a soft real-time system to improve and to optimise system operation during each decision period, lower-level controllers at supply/demand sides are modelled as hard real-time systems to maintain the stability. The two mentioned systems have different time granularities according to types of controlled objects and performance requirement. In the proposed microgrid, sustainable energy sources such as photovoltaic (PV) systems and wind turbines (WTs) are exploited as non-dispatchable prime movers of the mentioned system. The power grid is also used as a sustained power supply to support required point of common coupling (PCC) voltage regulation and system frequency. Other dispatchable dispersed generators within the residential section adjust their behaviours according to the power demand and reference signals received from RSEMS.

3 Mathematical model of the proposed system

Optimal energy management and power control in an integrated building and microgrid system can be defined as an optimisation problem with a number of objectives and different environmental/technical constraints as described below.

3.1 Distributed energy sources

3.1.1 Renewables: The generated power from renewables such as wind and solar is based on variable sources that fluctuate during the course of any given day or season. For example, the output power for a WT depends mainly on the local wind velocity and some other parameters as follows:

$$P_{\rm WT}(h) = C_{\rm p}(\lambda, \beta)(\rho A/2)V(h)^3, \quad \forall h \in T \tag{1}$$

Similarly, the available power from a PV system at any time h can be measured as

$$P_{\rm PV}(h) = Y_{\rm PV} f_{\rm PV}(G_{\rm T}(h)/G_{\rm T,STC})[1 + \alpha_{\rm p}(T_{\rm c}(h) - T_{\rm c,STC})], \quad \forall h \in T \tag{2}$$

3.1.2 Residential co-generation system (µCHP): In a µCHP with three subsystems including a fuel cell unit, an auxiliary boiler and a hot water storage tank (HWST), the electrical/thermal power outputs of the system can be calculated as follows: (see (3)) It is notable that the system's electrical and thermal outputs should be limited within a minimum stable generation and a maximum generation capacity limit as expressed in the third line of (3). Moreover, to avoid damaging the system, the electrical/thermal output of the unit should be changed by less than a certain amount over a period of time (known as the maximum ramp-rate constraints) which is considered in the last line of (3). Similar thermal power equation as stated in (3) together with related thermal constraints must be also considered for an auxiliary boiler.

The thermal behaviour of a HWST can be also modelled through the following equation considering the existing energy content of the system as well as all other thermal flows from/to the system

$$Q_{\rm st}(h+1) = Q_{\rm st}(h) + \left(P^{\rm th}_{\rm CHP}(h) + P^{\rm th}_{\rm aux}(h) - P^{\rm th}_{\rm D}(h) - P^{\rm th}_{\rm loss}(h)\right)\Delta h_{\rm step}, \quad \forall h \in T \tag{4}$$

Based on the above equation, the reservoir temperature during each time interval can be evaluated as stated in the following equation: (see (5))

3.1.3 Electrical energy storage system (EESS): EESS for residential applications can provide reliable back-up power in case of emergency and help regulate the power supply at homes. The behaviour of a BESS can be defined as a state of charge update function as shown below: (see (6)) For the technical reason, SOC which is defined as the fraction of the total energy (or battery capacity) that has been used over the total available from the battery should be limited within a lower and upper limits [line 3 in (6)]. In a similar way, for each BESS type, a particular set of restraints and conditions related to its charging and discharging power must be met [lines 4–5 in (6)].

3.2 Model of a residential building unit in thermal zone

3.2.1 Internal heat gain (IHG): The IHGs inside a building provide a valuable source of heat contribution to space heating. The main sources of IHG include people and household equipment (sensible and latent heat gain) as well as lights (sensible heat gain only). The heat output rate of human bodies depends on the level of activity and can be expressed as

$$\begin{aligned} Q_{\text{occ}}(h) &= \frac{A_{\text{cloth}}\left(T_{\text{skin}}(h) - T_{\text{eq}}(h)\right)}{R_{\text{cloth}} + (1/(h_{\text{conv}} + h_{\text{rad}}))} + \mu_{\text{evap}}\eta_{\text{fg}} \\ &= \frac{A_{\text{cloth}}\left(T_{\text{skin}}(h) - T_{\text{eq}}(h)\right)}{R_{\text{cloth}} + R_{\text{combined}}} + \mu_{\text{evap}}\eta_{\text{fg}}, \quad \forall h \in T \end{aligned} \tag{7}$$

where the first term on the right side of (7) estimates combined heat transfer in terms of convection and radiation from a clothed body to the environment and the second one denotes the evaporation heat dissipation.

The IHG from lighting in a building can be estimated by summing up the number of lights of each type (N_i) and wattage (W_i), and multiplying this number by related lighting utilisation (UF) and special allowance (SAF) factors as shown in the below equation:

$$Q_{\text{light}} = \sum_{i=1}^{k} N_i \times W_i \times \text{UF}_i \times \text{SAF}_i \times \text{SF}_i \tag{8}$$

In a same way, the heat gain from household equipment and appliances driven by electric motors within a conditioned space can be expressed as

$$Q_{\text{motor}} = P_{\text{n}} \times f_{\text{load}} \times f_{\text{usage}} / \eta_{\text{motor}} \tag{9}$$

For the cooking appliances, the heat gain can be calculated based on (10) considering recommended rates of radiant and convective heat dissipation from unhooded electric appliances during ready-to-cook conditions

$$Q_{\text{cook}} = P_{\text{n}} \times F_{\text{r}} \times F_{\text{u}} \tag{10}$$

For the rest of appliances, the peak heat gain can be taken as 50% of the total nameplate ratings of them [30, 31].

3.2.2 External heat gain (EHG): The sources for EHG of a building mainly include the heating system [such as a radiant floor heating/cooling system (RFH/CS)] and solar radiation. However, other external parameters such as wind speed can contribute to the heat loss of a building due to its effect on hybrid ventilation.

The thermal energy which is added (or removed) to (or from) a space by a heating (or cooling) system can be easily evaluated knowing the system's components and their functionalities. For example, in case of a RFH/CS, the heat output of the system can be measured as

$$\begin{aligned} &Q_{\text{RH}}(h) = (u_{\text{RH}}(h)\eta_H(h) - (1 - u_{\text{RH}}(h))\eta_C(h))P_{\text{RH}}(h), \quad \forall h \in T \\ &\text{s.t.} \\ &P_{\text{RH}} \in [0, \bar{P}_{\text{RH}}]; \quad \eta_H \in [\underline{\eta}_H, \bar{\eta}_H]; \quad \eta_C \in [\underline{\eta}_C, \bar{\eta}_C] \end{aligned} \tag{11}$$

The Sun has also a major effect on EHG of a building unit by the emission of long wavelength radiation. The solar heat gain of an exposed interior surface through a glazed area (such as the house floor on the sunny side) could be estimated as follows:

$$Q_{\text{sf}}(h) = \alpha_{\text{f}} A_{\text{f}} I(h), \quad \forall h \in T \tag{12}$$

Similarly, the heat exchange at the outside surfaces of a building which are subjected to the solar radiation (such as the exposed walls and the roof) can be evaluated as follows:

$$\begin{aligned} &P^{\text{e}}_{\text{CHP}}(h) = \frac{g_{\text{CHP}}(h)}{G_{\text{ref}}} \cdot \eta_{\text{e}} = P^{\text{th}}_{\text{CHP}}(h) \cdot \frac{\eta_{\text{e}}}{\eta_{\text{th}}}, \quad \forall h \in T \\ &\text{s.t.} \\ &P^{\text{e}}_{\text{CHP}}(h) \in [\underline{P}^{\text{e}}, \bar{P}^{\text{e}}]; \quad P^{\text{th}}_{\text{CHP}}(h) \in [\underline{P}^{\text{th}}, \bar{P}^{\text{th}}] \\ &\left|P^{\text{e}}_{\text{CHP}}(h) - P^{\text{e}}_{\text{CHP}}(h-1)\right| \le P^{\text{e}}_{\text{ramp}}; \quad \left|P^{\text{th}}_{\text{CHP}}(h) - P^{\text{th}}_{\text{CHP}}(h-1)\right| \le P^{\text{th}}_{\text{ramp}} \end{aligned} \tag{3}$$

$$\begin{aligned} T_{\text{st}}(h+1) = &\{(\text{HWD}(h)(T_{\text{cw}} - T_{\text{st}}(h)) + V_{\text{tot}}T_{\text{st}}(h))/V_{\text{tot}}\} + \left\{\left(P^{\text{th}}_{\text{CHP}}(h) + P^{\text{th}}_{\text{aux}}(h)\right)/(V_{\text{tot}}C_{\text{w}})\right\} \\ &- \{(A_{\text{st}}/(V_{\text{tot}}C_{\text{w}}R_{\text{st}}))(T_{\text{st}}(h) - T_{\text{b}}(h))\}, \quad \forall h \in T \\ \text{s.t.}& \\ T_{\text{st}}(h) \in &[\underline{T}_{\text{st}}, \bar{T}_{\text{st}}] \end{aligned} \tag{5}$$

$$\begin{aligned} &\text{SOC}(h+1) = \text{SOC}(h) + \left\{\left(\left(P^{\text{ch}}_{\text{BESS}}(h) - P^{\text{dch}}_{\text{BESS}}(h)\right)\Delta h_{\text{setp}}\right)/E_{\text{BESS}}\right\}, \quad \forall h \in T \\ &\text{s.t.} \\ &\text{SOC}(h) \in [\underline{\text{SOC}}, \overline{\text{SOC}}] \\ &P^{\text{ch}}_{\text{BESS}}(h) \le \overline{P}_{\text{ch}}\eta_{\text{ch}}u_{\text{BESS}}(h) \\ &P^{\text{dch}}_{\text{BESS}}(h)\eta_{\text{dch}} \le \overline{P}_{\text{dch}}(1 - u_{\text{BESS}}(h)) \end{aligned} \tag{6}$$

Table 1 Recommended values for heat transfer coefficients adjustment in different weather conditions

Weather conditions	Combined convection and radiation heat transfer coefficient, W/(m^2 °C)	
	Inner surfaces	Outer surfaces
winter (V_{wind} = 6.7 m/s)	8.29	34
summer (V_{wind} = 3.4 m/s)	8.29	22.7

$$Q_{\text{si}}(h) = \text{UA}_{\text{s}}\left(\left(T_{\text{out}}(h) + \frac{\alpha_{\text{s}} I(h)}{h_{\text{o}}} - \frac{\varepsilon\sigma\left(T_{\text{out}}^4(h) - T_{\text{surr}}^4(h)\right)}{h_{\text{o}}}\right) - T_{\text{in}}(h)\right), \quad \forall h \in T \tag{13}$$

Wind could also increase the heat losses of a building structure by affecting the convection heat transfer coefficient and the hybrid infiltration. Considering typical wind speed for winter and summer, recommended values for adjustment of the heat transfer coefficients for combined convection and radiation on the inner and outer surfaces of a building can be considered as shown in Table 1 [31].

Taking into consideration the above-mentioned IHGs and EHGs, the behaviour of a residential building unit in the thermal zone can be modelled as follows: (see (14) and (15)) (see (15))

3.3 Load scheduling potentials of household appliances

A household has different types of appliances with different characteristics such as energy demand, runtime and number of usages. While some of appliances cannot be scheduled or managed over the time and their functions are of direct use to the inhabitants, some others can be pre-programmed to run based on the user's preferences as well as the required operating parameters (ROP) and constraints as defined in the following equations: (see (16))

$$\sum_{h \in T_{\text{v},i}} s_i(h) = \text{RT}_i \tag{17}$$

$$\sum_{h \in T_{\text{v},i}} |s_i(h) - s_i(h-1)| \le 2 \tag{18}$$

$$\sum_{h \in T_{\text{v},j}} s_j(h) H\left(\lambda - \text{RT}_i + \sum_{\bar{h} = h_{\text{st}}}^{h} s_i(\bar{h})\right) = \text{RT}_j \tag{19}$$

$$P_{\text{D}}(h) = \sum_{k \in M} P_{\text{f,k}}(h) + \sum_{l \in N} P_{\text{s,l}}(h) s_{\text{l}}(h) \le \bar{P}_{\text{D}}, \quad \forall h \in T \tag{20}$$

where $h_{\text{st}} = \min(h_{\text{st},i}, h_{\text{st},j})$ and λ is a positive number smaller than 1. The first constraint as in (17) denotes that the operation of each schedulable task i must be done within an allowed time range with regard to its required run time. Constraint (18) enforces the continuous operation of those appliances that are not allowed to be turned off or set to standby during their run times. Requirements for successive operation of some in-home devices (e.g. a tumble dryer as task j and a washing machine as task i) are imposed by (19), while constraint for the maximum power consumption of a house is set by (20).

3.4 Objective functions

In this work, two different objective functions are taken into account for optimal energy management and task scheduling in a grid-tied residential microgrid. The first one, which deals with the total operation cost (TOC) minimisation, is expressed as follows:

$$\text{Min:TOC} = \sum_{h \in T} \left\{\text{RTP}(h) P_{\text{grid}}(h) + \rho_{\text{gas}} (u_{\text{CHP}}(h) g_{\text{CHP}}(h) + u_{\text{aux}}(h) g_{\text{aux}}(h))\right\} \tag{21}$$

The first term at the right side of (21) denotes cost of electricity exchanged with the power grid at a given time h and the second term shows the natural gas consumption cost for a given building.

The second objective function aims at maximising the user's convenience and comfort level (UCCL) as follows:

$$\text{Max:UCCL} = \xi_1 \sum_{h \in T} \sum_{i \in N} (\psi \text{ID}_i \text{SL}_i(h)) + \xi_2 \sum_{h \in T} \gamma \text{CL}(h) \tag{22}$$

in which $\text{SL}_i(h)$ and $\text{CL}(h)$ are defined as the user's satisfaction degree about in-home task scheduling ([26, 29, 32]) and occupant's thermal comfort level ([26, 33]), respectively, and are quantified based on the distribution functions shown in Fig. 2. As it can be seen in the same figure, from a user's viewpoint, the degree of satisfaction reaches the maximum value (e.g. $\text{SL}_i = 1$) when task i is operated within its defined DOI_i range, and it decreases to zero gradually as it goes beyond the desired range. In a similar way, as long as the indoor temperature is kept within the comfort range ($T_{\text{set}} \pm \Delta T_{\text{th}}$), CL would be quantified as ‘1’ denoting that the occupants are fully satisfied with the thermal zone; otherwise it will be assigned lower values. It should be noted that the trade-off between SL and CL functions can be easily modified using ξ_1 and ξ_2 weighting factors while their shape of distribution can be adjusted through the penalty factors ψ and γ, respectively. Considering the above defined objective functions, the hybrid optimisation model is formulated as

$$\text{Min: Mob}\, j = \text{TOC}\,\text{UCCL}^{-1} \tag{23}$$

subject to the following power balance equation and those stated in (3)–(20)

$$\begin{aligned} &T_{\text{in}}(h) = T_{\text{in}}(h-1) + \Delta h_{\text{step}} \left(\frac{Q_{\text{fi}}(h) + Q_{\text{si}}(h) + Q_{\text{ihg}}(h) - Q_{\text{io}}(h)}{m_i c_{\text{p},i}}\right), \quad \forall h \in T \\ &\text{s.t.} \\ &\underline{T}_{\text{in}} \le T_{\text{in}}(h) \le \bar{T}_{\text{in}} \end{aligned} \tag{14}$$

$$\begin{aligned} &T_{\text{f}}(h) = T_{\text{f}}(h-1) + \Delta h_{\text{step}} \left(\frac{Q_{\text{RH}}(h) + Q_{\text{sf}}(h) - Q_{\text{fg}}(h) - Q_{\text{fi}}(h)}{m_{\text{f}} c_{\text{p,f}}}\right), \quad \forall h \in T \\ &\text{s.t.} \\ &\underline{T}_{\text{f}} \le T_{\text{f}}(h) \le \bar{T}_{\text{f}} \end{aligned} \tag{15}$$

$$\text{ROP}_i = \begin{bmatrix} \{[h_{\text{st},i}, h_{\text{et},i}]\text{: start} - \text{end time period}\}, \{\text{RT}_i\text{: runtime}\}, \{\text{ID}_i\text{: task priority}\} \\ \{\text{DOI}_i = [h_{\text{ds},i}, h_{\text{de},i}]\text{: desired operating time}\}, \{P_{\text{s},i}\text{: power demand}\} \end{bmatrix}, \quad \forall i \in N \tag{16}$$

$$P_{\mathrm{grid}}(h) + P^{\mathrm{e}}_{\mathrm{CHP}}(h) + \delta \cdot (P_{\mathrm{WT}}(h) + P_{\mathrm{PV}}(h)) - P_{\mathrm{BESS}}(h) = P_{\mathrm{D}}(h), \quad \forall h \in T \tag{24}$$

where δ denotes the energy share of each household from sustainable energy sources within the residential microgrid according to the ratios of investment.

3.5 Master–slave control of energy sources

The lower-level control structure (here named as 'master–slave') of the existing DG sources is depicted in Fig. 3.

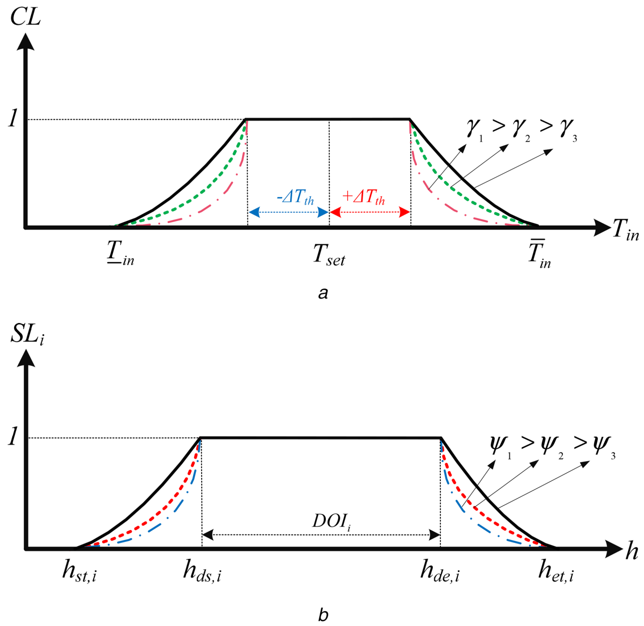

Fig. 2 *Definition of user's satisfaction level and thermal comfort level*
(a) Thermal comfort level, *(b)* Satisfaction degree

Based on this control structure, each controllable DG is treated as a 'grid-following' unit and operated in power control mode (PCM) to follow a power reference (P^*), while the utility (which is the master unit) is operated in grid-forming mode (VCM) to maintain the voltage and the frequency within the range. In this regard, droop control is implemented based on (25) and (26) in primary loop for the master unit, and reverse droop controller is utilised for the slave units as expressed in (27)

$$\omega = \omega^* - m_{\mathrm{d}} P \tag{25}$$

$$E = E^* - n_{\mathrm{d}} Q \tag{26}$$

$$Q^* = (1/n_{\mathrm{r}}) \cdot (E^* - E_{\mathrm{g}}) \tag{27}$$

It should be mentioned that within the proposed structure, the inner-loop control of VCM aims at achieving good output voltage regulation with respect to determined capacitor voltage reference while the inner-loop control of PCM regulates the output power. For both inner loops typical proportional–integral controllers are appropriately designed and used. In the primary control loops, low-pass filters are also applied to limit the loop bandwidth, so that the primary control can be separately designed and the inner loop of VCM and PCM can be considered as ideal voltage and current sources, respectively [32].

4 Simulation results and discussions

The performance of the proposed optimal dispatching model is evaluated through different simulation case studies and relevant results analysis. As shown in Fig. 1, the case study is configured as an integrated building and grid-tied microgrid system with operating parameters described in Table 2 and shown in Fig. 4. The building unit design and construction characteristics are also adopted from [33]. With regards to the proposed lower-level control structure of the dispatchable DG sources, the control system parameters are shown in Table 3. For the examined

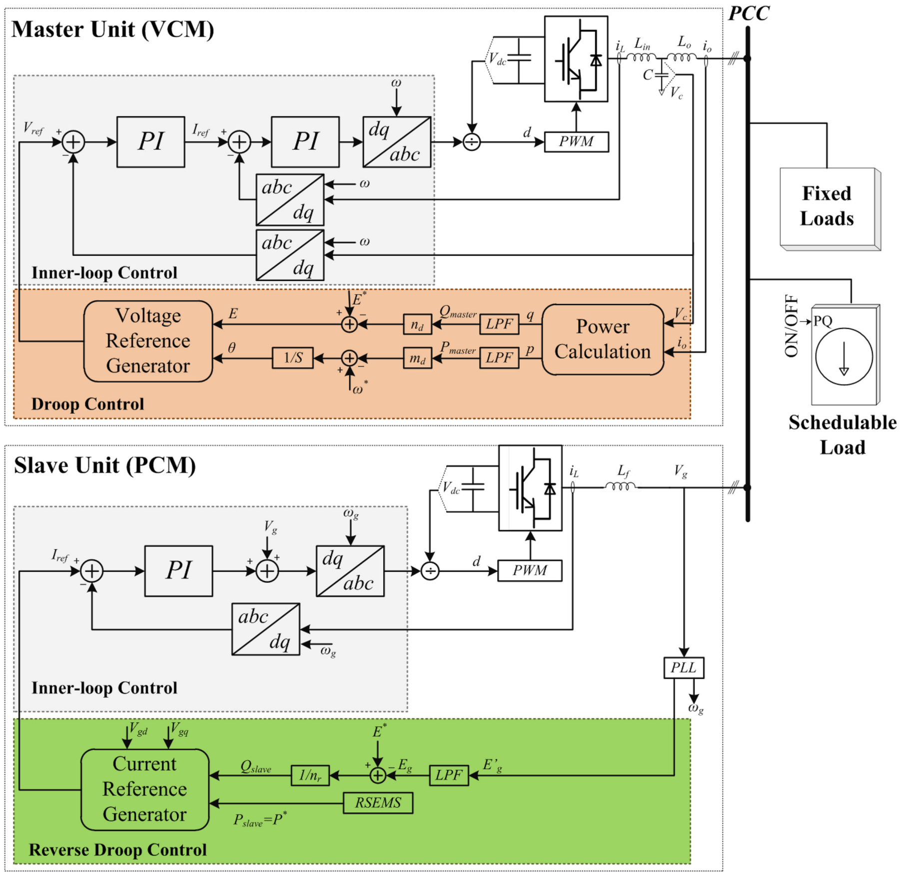

Fig. 3 *Master–slave control of distributed energy sources*

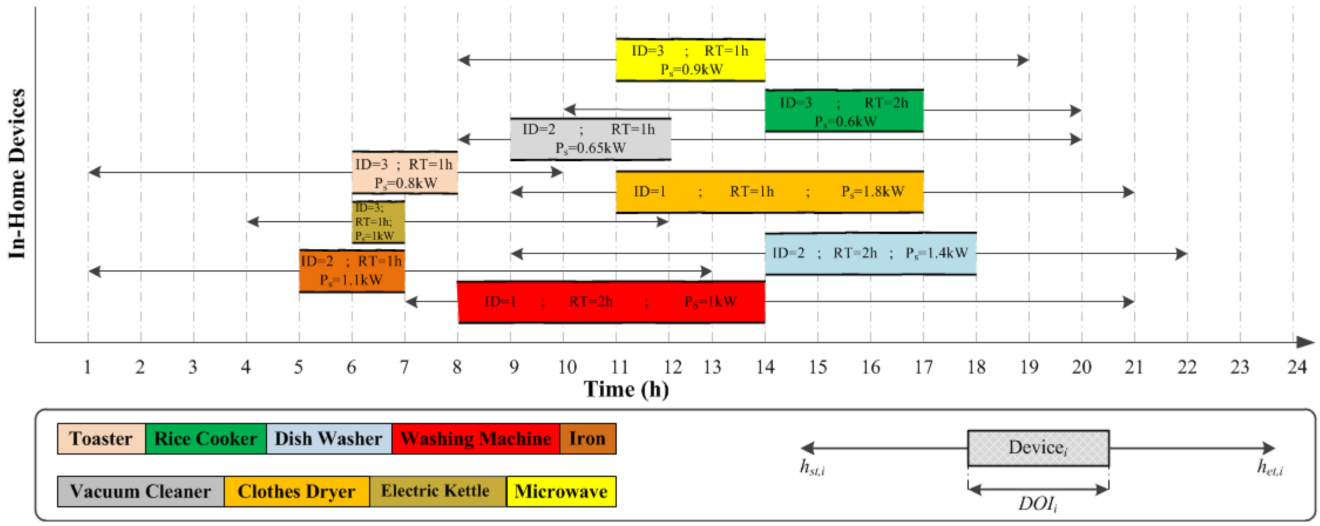

Fig. 4 *Schedulable tasks data and user's preferences*

Table 2 Specifications of the energy sources within the residential microgrid [29, 36–38]

Parameter	Value	Unit	Parameter	Value	Unit
WT generator					
ρ	1.18	kg/m^3	A	120	m^2
v_{survival}	60	m/s	D_{rotor}	12.35	m
PV system					
Y_{PV}	0.25	kW	f_{PV}	77	%
$G_{\text{T,STC}}$	1	kW/m^2	$T_{\text{c,STC}}$	25	°C
α_{p}	−0.44	%/°C			
Residential μCHP					
$\underline{P}^{\text{e}}, \bar{P}^{\text{e}}$	0.3, 1.5	kW	$\underline{P}^{\text{th}}_{\text{aux}}, \bar{P}^{\text{th}}_{\text{aux}}$	4,19	kW
$P^{\text{e}}_{\text{ramp}}$	0.9	kW/h	V_{tot}	200	l
g_{CHP}	92.4 × 10^{-3}	m^3/h	A_{st}	1.99	m^2
$\eta_{\text{e}}, \eta_{\text{th}}, \eta_{\text{aux}}$	30,70, 86	%	R_{st}	2.818	m^2 °C/W
$\bar{T}_{\text{st}}, \underline{T}_{\text{dch}}$	60, 80	°C	T_{cw}	10	°C
Battery-based EESS					
E_{BESS}	24	kWh	$\underline{SOC}, \overline{SOC}$	20–80	%
$\bar{P}_{\text{ch}}, \underline{P}_{\text{dch}}$	3.3, 3.3	kW	$\eta_{\text{ch}}, \eta_{\text{dch}}$	87, 90	%
RFH/CS					
$\bar{P}_{\text{RH}}$	2	kW	T_{set}	25	°C
$\underline{\eta}_H, \bar{\eta}_H$	100, 400	%	$\underline{\eta}_C, \bar{\eta}_C$	100, 300	%
$\Delta T_{\text{th, hot}}$	±3	°C	$\Delta T_{\text{th, cold}}$	±2	°C

Table 3 Master–slave control system parameters

Type	Parameters	Symbol	Value	Unit
electrical parameters	rated PCC voltage	V^*	230	V
	system frequency	f^*	50	Hz
	LCL filter capacitance	C	2200	μF
	VCM filter inductance	L_{in}	1.8	mH
	PCM filter inductance	L_{f}	3.6	mH
	output impedance	L_{o}	0.1	mH
inner loops and droop control	voltage proportional term	k_{pV}	0.1	–
	voltage integral term	k_{iV}	200	s^{-1}
	current proportional term	k_{pI}	15	–
	current integral term	k_{iI}	50	s^{-1}
	frequency droop	m_{d}	0.003	rad/ s/W

residential section and according to the demand profile of the household loads as well as its occupancy behaviour, the IHG is also estimated based on (7)–(10) to be 3.5 W/m^2.

Likewise, the maximum allowable power exchange between the utility and the house under RTP is limited to 5.5 kW during each time slot. Other required data such as meteorological information and energy prices for the study time and location are also collected from [39–41]. It should be mentioned that the simulation platform is implemented in MATLAB Simulink® and General Algebraic Modeling System (GAMS) is incorporated as computation engine for optimisation tasks.

Fig. 5 illustrates the performance comparison of the proposed RSEMS with a conventional EMS (CEMS) in terms of different objectives. It is noteworthy that a CEMS schedules in-home tasks economically and keeps the indoor temperature within the comfort zone [i.e. ξ_2 is set to unity in (22)]; however, it does not consider user's preferences in energy scheduling [i.e. ξ_1 is set to zero in (22)].

It is clearly observed from case-study simulations that the proposed methodology outperforms the conventional way of energy management. In case of a CEMS, although it collects the RTP information and realises a penny-wise dispatch pattern to lowering down the energy costs, it fails to meet the user's satisfaction. On the other hand, the hybrid objective function (Mob *j*) that includes both energy cost and comfort levels improves considerably (up to 29 and 33% in hot and cold weather conditions, respectively) using the proposed RSEMS. It can be also seen from the numerical results that the performances of RSEMS and CEMS are very competitive to one another in terms of energy consumption cost reduction, which implies that RSEMS has the capability to dispatch the schedulable consumption and generation in a way not only to conserve energy within the building, but also to fulfil the inhabitants' needs in terms of UCCL index. It is also noteworthy that the running time of the proposed model is <4 s under different operating conditions, which makes it applicable for a real EMS system with selective time intervals from 1 min to 1 h. It can be also understood from the results that RSEMS optimal portfolio slightly changes in the hot and cold weather conditions, mainly because of the building IHG as well as EHGs, which in turn affects the cooling/heating capacity of the system and energy management policy of the controllers.

To have a better understanding of the proposed EMS performance, computer simulations regarding optimal operation management of schedulable tasks and DG units are depicted in Fig. 6 for a hot summer day. As it can be observed from the optimised dispatch profile, operating behaviours of the units change during different times of a given day. For example, when the electricity price is relatively low, the power grid supplies majority of the residential demand and the BESS is charged accordingly with lower cost. However, during peak-price hours the controllable DGs are involved more in the generation mix not only to supply the load economically, but also to sell extra power into the power grid for making more profits. On the demand side, the operating times of the tasks are also scheduled in a way to meet both the constraints and the user's objectives. As an illustration, for two household appliances such as washing machine and tumble dryer, the successive operation is planned effectively by RSEMS to meet the user's preferences as defined in (16) and (22) and shown in Fig. 4, and to satisfy the requirements enforced by (17), (19) and (20).

In this case study, the lower-level master–slave control of the energy sources is also enabled effectively in coordination with the system-level optimisation. As can be seen in Fig. 7, the power utility, which serves as a grid-forming unit, keeps the frequency within an acceptable range and holds a good output voltage regulation by the use of dedicated controllers; however, other available controllable DGs that paly as slave units try to regulate their output powers based on the reference signals received from the RSEMS.

Fig. 8 shows the simulation results for the case where the μCHP system is optimally controlled to meet the hot water needs of the residents in a given day. Likewise, Fig. 9 illustrates the performance of the proposed optimal model as applied to the heating/cooling scenarios for the given building in different weather conditions. From the related simulations, it is observed that the operations of RFH/CS and μCHP systems are managed optimally by the RSEMS with regards to the user's comfort level, hot water needs and the existing constraints for these units.

The thermal behaviour of the building in different weather conditions is illustrated in Fig. 9. As it can be observed, heat can be easily exchanged between the indoor air and the outdoor environment based on the temperature differences in these nodes, which in turn affects the heating/cooling load of the building.

For example in summer time and during hot days, not only the heat from the direct sunlight warms up the house [by increasing Q_{sf}

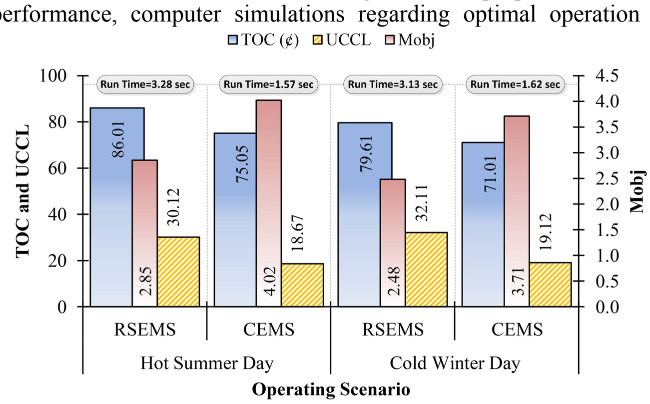

Fig. 5 *Performance of the proposed RSEMS against CEMS under different simulation case studies*

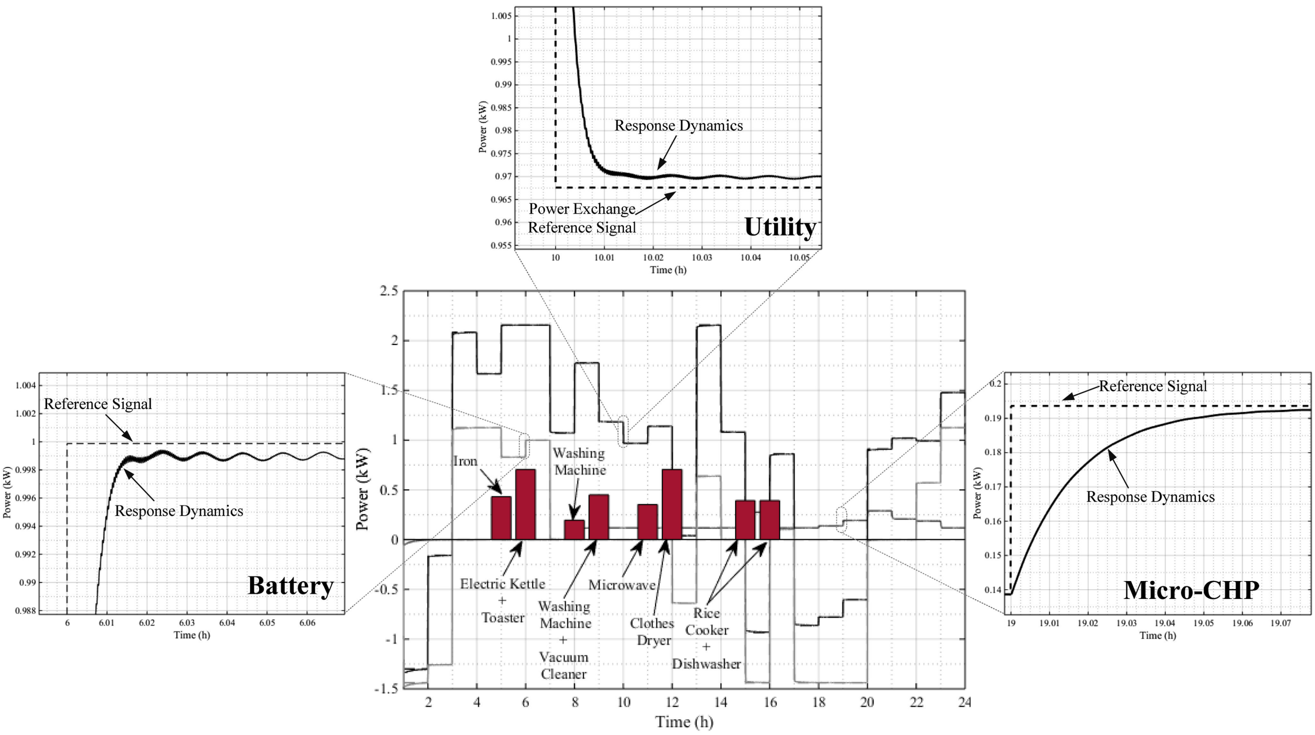

Fig. 6 *Optimised dispatch and control of household devices and DGs using the proposed methodology*
(a) Frequency, ***(b)*** Three-phase voltage

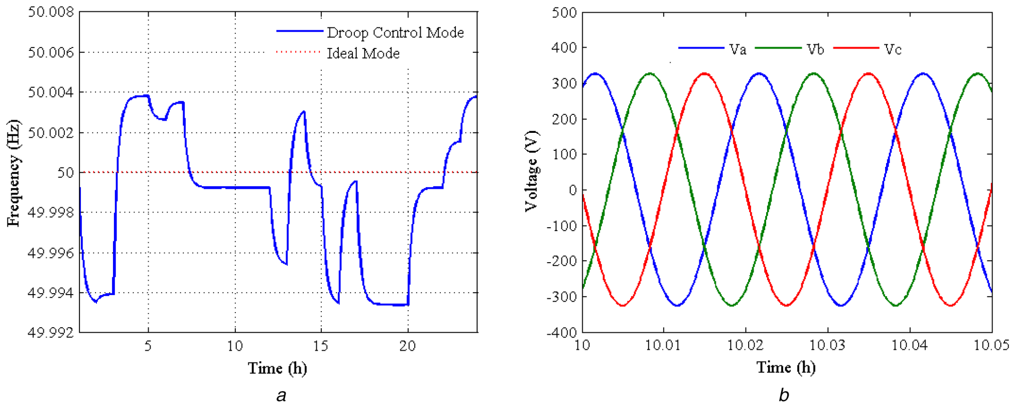

Fig. 7 *Performance evaluation of the master controller*
(a) System frequency, ***(b)*** Voltage magnitude at PCC

heat flow as described in (12) and accordingly increasing the floor temperature based on (15)], but also the thermal flows from the exposed exterior surfaces such as walls and the roof will contribute to the heat gain of the building all day long (i.e. Q_{si} heat flow in

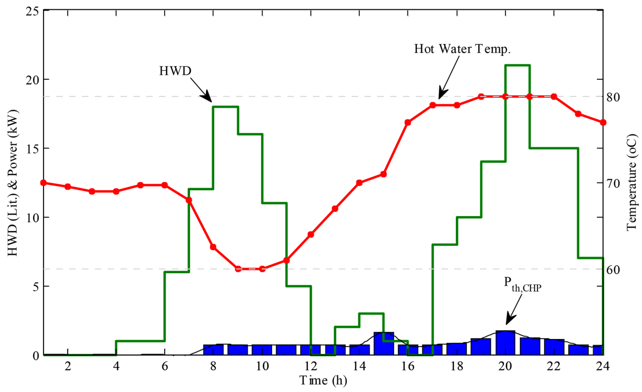

Fig. 8 *Operation of the µCHP based on the hourly hot water demand*

Fig. 9). For this reason, the RFH/CS operates more in the cooling mode (i.e. negative $Q_{\rm fi}$ heat flow which denotes heat absorption by the floor through cooling operation of the RFH/CS system) to satisfy the desired body comfort. On the contrary, due to the lower outside temperature in winter times (see temperature profiles in Fig. 9*b*), most of the heat is transferred through the building structures to the outdoor ambient (i.e. positive $Q_{\rm io}$ and $Q_{\rm fo}$ heat flows) thus enforcing the RFH/CS to produce more heat (i.e. positive $Q_{\rm fi}$ heat flow) and to keep the thermal comfort range for the inhabitants (i.e. the operative indoor temperature range of 23–27°C as defined by user). It is noteworthy that in such weather condition, both the IHGs and EHGs of the building are contributing positively to the heat gain of the building during the day and therefore mitigating the running cost of the system for heating purposes. This can be easily understood from Fig. 9 by comparing the RFH/CS performance during the study period under different weather conditions in terms of the total operating times and the energy consumption. It should be noted that the IHG has been estimated based on (7)–(10) to be 3.5 W/m^2 of floor area averaged

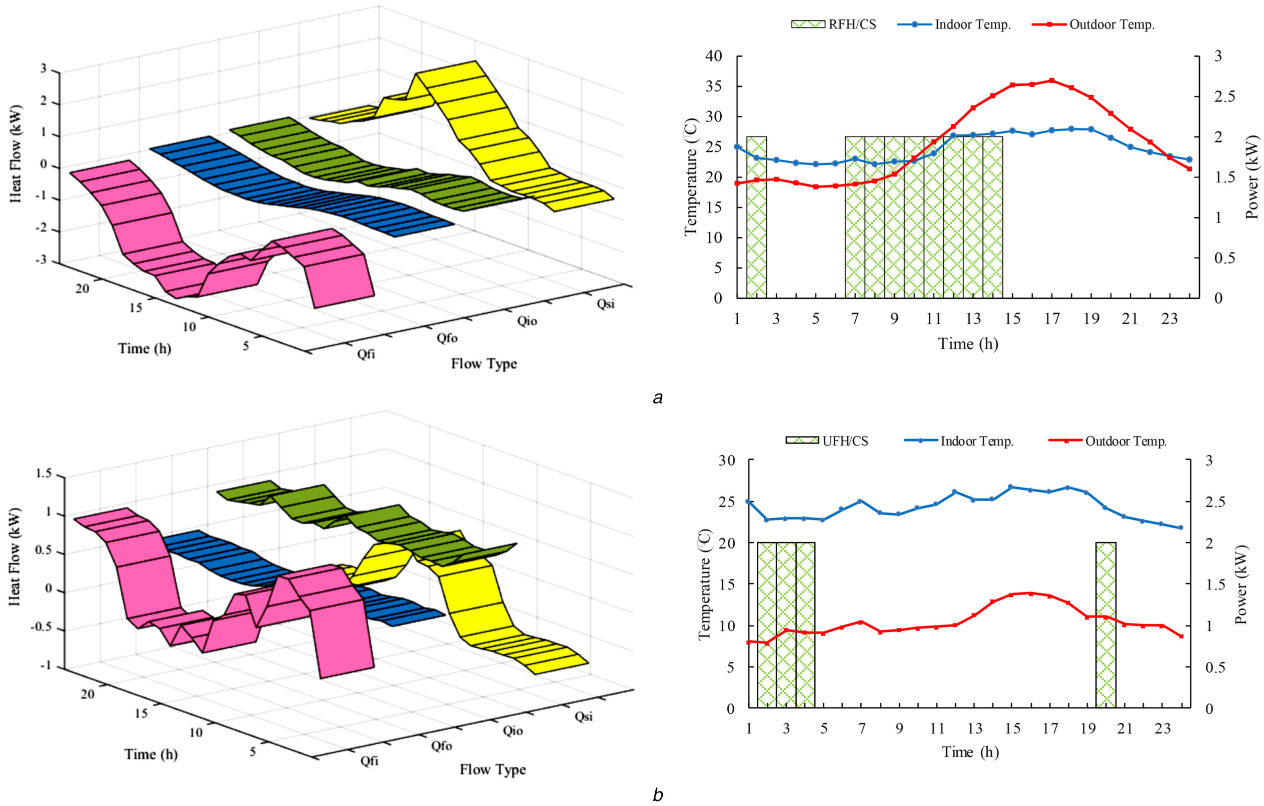

Fig. 9 *Heat flows and optimal operation of RFH/CS system during different weather conditions*
(a) Hot summer day, ***(b)*** Cold winter day

over the study period according to the demand profile of the examined household loads and occupancy.

5 Conclusion and future works

In this paper, an efficient EMS for applications in sustainable buildings and microgrid system was described, mathematically modelled and validated in different operating conditions. The proposed framework which was developed as integration of a system-level optimiser and lower-level controllers, encompassed various thermal/electrical models for heat exchange within a residential building as well as load scheduling potentials of household appliances with associated constraints. Moreover, it integrated different means of heat and electricity generation into a residential microgrid and provided an optimal dispatch model of the corresponding units under various working scenarios. It was demonstrated through the computer simulations that the proposed EMS has the capability to reduce domestic energy usage and improve the user's satisfaction degree and comfort level taking into account real-time system's constraints and deadlines. Compared with a CEMS, the proposed scheme could also track the electricity usage by the hour and find the most efficient solution to supply the demand and/or shift (load) activities into time frames when the user's utility is the highest.

Further research is needed to investigate more real smart buildings settings and preferences. We also need to study and exploit suitable statistical models of uncertain parameters and apply them in operation management of residential microgrids in order to make the best decisions on average. Moreover, there is a need to incorporate error handling mechanisms to anticipate, detect and resolve errors during metering, sensing and communication processes. In future works, we will also carry out more experiments on larger test systems and investigate the effectiveness of our proposed architecture in a multi-agent-based simulation environment.

6 References

[1] GEA: '*Global energy assessment – toward a sustainable future*' (Cambridge University Press, Cambridge, UK and New York, NY, USA and the International Institute for Applied Systems Analysis, Laxenburg, Austria, 2012)

[2] Anvari-Moghaddam, A., Mokhtari, G., Guerrero, J.M.: 'Coordinated demand response and distributed generation management in residential smart microgrids', in Mihet, D.E.L. (Ed.): '*Energy management of distributed generation systems*' (InTech Open Access Publishers, 2016), doi: 10.5772/63379

[3] Rodriguez-Diaz, E., Vasquez, J.C., Guerrero, J.M.: 'Intelligent DC homes in future sustainable energy systems: when efficiency and intelligence work together', *IEEE Consum. Electron. Mag.*, 2016, **5**, (1), pp. 74–80

[4] Mokhtari, G., Anvari-Moghaddam, A., Nourbakhsh, G.: 'Distributed control and management of renewable electric energy resources for future grid requirements', in Mihet, D.E.L. (Ed.): '*Energy management of distributed generation systems*' (InTech Open Access Publishers, 2016), doi: 10.5772/63379

[5] Pavan Kumar, Y.V., Bhimasingu, R.: 'Review and retrofitted architectures to form reliable smart microgrid networks for urban buildings', *IET Netw.*, 2015, **4**, (6), pp. 338–349

[6] Sivaneasan, B., Nandha Kumar, K., Tan, K.T.*, et al.*: 'Preemptive demand response management for buildings', *IEEE Trans. Sustain. Energy*, 2015, **6**, (2), pp. 346–356

[7] Lampropoulos, I., Garoufalis, P., van den Bosch, P.P.J.*, et al.*: 'Hierarchical predictive control scheme for distributed energy storage integrated with residential demand and photovoltaic generation', *IET Gener. Transm. Distrib.*, 2015, **9**, (15), pp. 2319–2327

[8] Karami, H., Sanjari, M.J., Hosseinian, S.H.*, et al.*: 'An optimal dispatch algorithm for managing residential distributed energy resources', *IEEE Trans. Smart Grid*, 2014, **5**, (5), pp. 2360–2367

[9] Anvari-Moghaddam, A., Vasquez, J.C., Guerrero, J.M.: 'Load shifting control and management of domestic microgeneration systems for improved energy efficiency and comfort'. 41st Annual Conf. IEEE Industrial Electronics Society, Yokohama, 2015, pp. 96–101

[10] Yuan, W., Lau, V.K.N., Tsang, D.H.K.*, et al.*: 'Optimal energy scheduling for residential smart grid with centralized renewable energy source', *IEEE Syst. J.*, 2014, **8**, (2), pp. 562–576

[11] Kuzlu, M.: 'Score-based intelligent home energy management (HEM) algorithm for demand response applications and impact of HEM operation on customer comfort', *IET Gener. Transm. Distrib.*, 2015, **9**, (7), pp. 627–635

[12] Chen, C., Duan, S., Cai, T.*, et al.*: 'Smart energy management system for optimal microgrid economic operation', *IET Renew. Power Gener.*, 2011, **5**, (3), pp. 258–267

[13] Anvari-Moghaddam, A., Dragicevic, T., Vasquez, J.C.*, et al.*: 'Optimal utilization of microgrids supplemented with battery energy storage systems in grid support applications'. 1st IEEE Int. Conf. DC Microgrids (ICDCM), 2015, Atlanta, GA, pp. 57–61

[14] Vivekananthan, C., Mishra, Y., Li, F.: 'Real-time price based home energy management scheduler', *IEEE Trans. Power Syst.*, 2015, **30**, (4), pp. 2149–2159

[15] Ma, J., Chen, H.H., Song, L.*, et al.*: 'Residential load scheduling in smart grid: a cost efficiency perspective', *IEEE Trans. Smart Grid*, 2016, **7**, (2), pp. 771–784

[16] Li, L., Mu, H., Gao, W.*, et al.*: 'Optimization and analysis of CCHP system based on energy loads coupling of residential and office buildings', *Appl. Energy*, 2014, **136**, pp. 206–216

[17] Chen, C., Wang, J., Heo, Y.*, et al.*: 'MPC-based appliance scheduling for residential building energy management controller', *IEEE Trans. Smart Grid*, 2013, **4**, (3), pp. 1401–1410

[18] Qayyum, F.A., Naeem, M., Khwaja, A.S.*, et al.*: 'Appliance scheduling optimization in smart home networks', *IEEE Access*, 2015, **3**, pp. 2176–2190

[19] Chen, X., Wei, T., Hu, S.: 'Uncertainty-aware household appliance scheduling considering dynamic electricity pricing in smart home', *IEEE Trans. Smart Grid*, 2013, **4**, (2), pp. 932–941

[20] Rasheed, M.B., Javaid, N., Ahmad, A.*, et al.*: 'An efficient power scheduling scheme for residential load management in smart homes', *Appl. Sci.*, 2015, **5**, pp. 1134–1163

[21] Anvari-Moghaddam, A., Monsef, H., Rahimi-Kian, A.: 'Optimal smart home energy management considering energy saving and a comfortable lifestyle', *IEEE Trans. Smart Grid*, 2015, **6**, (1), pp. 324–332

[22] Yoon, J.H., Baldick, R., Novoselac, A.: 'Dynamic demand response controller based on real-time retail price for residential buildings', *IEEE Trans. Smart Grid*, 2014, **5**, (1), pp. 121–129

[23] Brahman, F., Honarmand, M., Jadid, S.: 'Optimal electrical and thermal energy management of a residential energy hub, integrating demand response and energy storage system', *Energy Build.*, 2015, **90**, pp. 65–75

[24] Mao, M., Jin, P., Hatziargyriou, N.D.*, et al.*: 'Multiagent-based hybrid energy management system for microgrids', *IEEE Trans. Sustain. Energy*, 2014, **5**, (3), pp. 938–946

[25] Parvizimosaed, M., Farmani, F., Anvari-Moghaddam, A.: 'Optimal energy management of a micro-grid with renewable energy resources and demand response', *J. Renew. Sustain. Energy*, 2013, **5**, (5), pp. 31–48

[26] Anvari-Moghaddam, A., Monsef, H., Rahimi-Kian, A.: 'Cost-effective and comfort-aware residential energy management under different pricing schemes and weather conditions', *Energy and Build.*, 2015, **86**, pp. 782–793

[27] Wei, Q., Liu, D., Shi, G.*, et al.*: 'Multibattery optimal coordination control for home energy management systems via distributed iterative adaptive dynamic programming', *IEEE Trans. Ind. Electron.*, 2015, **62**, (7), pp. 4203–4214

[28] Lee, S., Kwon, B., Lee, S.: 'Joint energy management system of electric supply and demand in houses and buildings', *IEEE Trans. Power Syst.*, 2014, **29**, (6), pp. 2804–2812

[29] Anvari-Moghaddam, A., Monsef, H., Rahimi-Kian, A.*, et al.*: 'Optimized energy management of a single-house residential micro-grid with automated demand response'. 2015 IEEE Eindhoven PowerTech, Eindhoven, 2015, pp. 1–6

[30] Bansal, N.K., Hauser, G., Minke, G.: '*Passive building design*' (Elsevier Science, New York, 1994)

[31] 'ASHRAE Handbook-Fundamentals' (American Society of Heating, Refrigerating and Air-Conditioning Engineers Publishers, Inc., Atlanta, GA, USA, 2001)

[32] Jiang, B., Fei, Y.: 'Dynamic residential demand response and distributed generation management in smart microgrid with hierarchical agents', *Energy Procedia*, 2011, **12**, pp. 76–90

[33] Fanti, M.P., Mangini, A.M., Roccotelli, M.*, et al.*: 'A district energy management based on thermal comfort satisfaction and real-time power balancing', *IEEE Trans. Autom. Sci. Eng.*, 2015, **12**, (4), pp. 1271–1284

[34] Wu, D., Tang, F., Dragicevic, T.*, et al.*: 'A control architecture to coordinate renewable energy sources and energy storage systems in islanded microgrids', *IEEE Trans. Smart Grid*, 2015, **6**, (3), pp. 1156–1166

[35] Bambrook, S.M., Sproul, A.B., Jacob, D.: 'Design optimization for a low energy home in Sydney', *Energy Build.*, 2011, **43**, (7), pp. 1702–1711

[36] Morphic Technologies AB: 'Small wind turbine for professional use', Doc no. 09–027 B, SWT 20 Data Sheet. Available at http://www.morphic.com, accessed 12 May 2013

[37] Hyundai Heavy Industries Co. Ltd: 'Hyundai solar module'. Available at http://www.hyundaisolar.com, accessed 12 May 2013

[38] Panasonic Corporation, Viessman Group: 'Panasonic and Viessmann to sell Europe's first fuel cell cogeneration system for homes'. Available at http://news.panasonic.com/global/press/data/2013/09/en130910-4/en130910-4.html, accessed 15 May 2013.

[39] Compressed Natural Gas (CNG) Systems. Available at http://www.oes.net.au, accessed 15 October 2013

[40] Climate Data Online. Available at http://www.bom.gov.au, accessed 2 August 2015

[41] Electricity Price & Demand. Available at: http://www.aemo.com.au, accessed 17 September 2015